Electronic Supplementary Information for

Superhydrophilic phosphate and amide functionalized magnetic adsorbent: a new combination of anti-biofouling and uranium extraction from seawater

Xuejie Guo[a,b], Rongrong Chen[a,b,*], Qi Liu[a,b], Jingyuan Liu[a,b], Hongsen Zhang [a,b,c], Jing Yu[a,b], Rumin Li [a,b,c] Milin Zhang[a,b] and Jun Wang[a,b,c,*]

[a] *Key Laboratory of Superlight Material and Surface Technology, Ministry of Education, Harbin Engineering University, Harbin 150001, China.*

[b] *College of Materials Science and Chemical Engineering, Harbin Engineering University, 150001, PR China.*

[c] *Harbin Engineering University Capital Management Co., Harbin 150001, China.*

**Correspondence authors: Tel: +86 451 8253 3026. Fax: +86 451 8253 3026. E-mail addresses:*
chenrongrong95@163.com (Rongrong Chen); zhqw1888@sohu.com (Jun Wang)

SI.1 Characterization

The morphology and structure of the microspheres were characterized by a field emission scanning electron microscope (SEM, Hitachi S4800) and transmission electron microscope (TEM, JEOL, JEM-2010). Fourier-transform infrared (FTIR) spectra of the microspheres were recorded to analyze the surface characteristics of the nanocarriers on an AVATAR 360 FTIR spectrophotometer in the 400–4000 cm^{-1} region by using the KBr-disk method. The X-ray diffraction (XRD) patterns were taken in a Rigaku D/max-IIIB diffractometer (Tokyo) using nickel-filtered Cu K$_{\alpha}$ radiation at 40 kV, 150 mA. X-ray photoelectron spectroscopy (XPS) measurements were performed using a PHI 5700 ESCA spectrometer with Al KR radiation (h$_{\nu}$= 1486.6 eV). The magnetic properties of the composite microspheres were measured via vibrating sample magnetometry (VSM JDM-13) at room temperature. Inductive Coupled Plasma (ICP, Bruker 820-MS)

SI.2 Effect of contact time and kinetics study on the adsorption of U (VI) on Fe_3O_4, FCS and FCCP composites

As the sorption kinetics govern the residence time of the sorption reaction and determine the solute uptake rate or the efficiency of the reaction, the following pseudo-first-order, pseudo-second-order and Weber-Morris (W-M) models are employed to interpret the mechanism controlling the sorption process. The linear form of the two models can be expressed by the following Eqs. S1-S3:

$$\ln\left(q_e - q_t\right) = lnq_e - k_1 t \qquad \text{(S1)}$$

$$\frac{t}{q_t} = \frac{1}{k_2} \cdot q_e^2 + \frac{t}{q_e} \qquad \text{(S2)}$$

$$q_e = K_{ip}\sqrt{t} + C \qquad \text{(S3)}$$

Where q_t and q_e (mg g^{-1}) are the capacity of U (VI) at time t (min) and at equilibrium, K_{ip} is internal diffusion constant, respectively, and k_1 (min^{-1}) and k_2 (g mg^{-1} min^{-1}) are the respective rate constants.

SI.3 Effect of initial concentration and volume of U (VI) solution, adsorption isotherms study on the adsorption of U(VI) on FCS and FCCP composites

To further explore the treatment capability of adsorbents, the effect of initial concentration and volume of U (VI) was investigated; subsequently, the adsorption isotherms were studied to probe the maximum adsorption capacity and the progress of adsorption. The adsorption of U (VI) on the FCS and FCCP composites increased with increasing temperature and the Langmuir, Freundlich and Dubinin-Radushkevich model models were applied to simulate experimental data.

$$C_e/q_e = 1/b \cdot q_m + C_e/q_m \qquad \text{(S4)}$$

$$\ln q_e = \ln k + 1/nlnC_e \qquad \text{(S5)}$$

$$\ln q_e = ln\, q_m - \ \beta\varepsilon^2 \qquad \text{(S6)}$$

$$\varepsilon = RTln\left(1 + 1/C_e\right) \qquad \text{(S7)}$$

Where C_e (mg L^{-1}) is the equilibrated U (VI) concentration, q_e (mg g^{-1}) is the amount of U(VI) adsorbed on the adsorbents capacity at equilibrium. K (L mg^{-1}) is a Langmuir constant related to the energy of the adsorbent and q_m (mg g^{-1}) is the saturation capacity at complete monolayer coverage. β is the activity coefficient and ε is the Polanyi potential.

Based on these isotherm behaviour findings, we examined the thermodynamics on the sorption of U (VI) onto FCS and FCCP composites. The following equations were used to calculate these thermodynamic parameters:

$$\ln K_D = \frac{\Delta S^\circ}{R} - \frac{\Delta H^\circ}{RT} \qquad \text{(S8)}$$

$$\Delta G^o = \Delta H^o - T\Delta S^o \qquad \text{(S9)}$$

$$K_D = \frac{q_e}{C_e} = \frac{(C_o - C_e)}{C_e} \cdot \frac{V}{m} \qquad \text{(S10)}$$

Where K_D is the distribution ratio of the U (VI).

SI.4 Effect of co-existing ions on FCCP adsorbents

The selectivity coefficient (S_U) for U (VI), is defined as a specific term to describe the potency and degree of selectivity of the adsorbents as follows:

$$S_U = \frac{K_D^U}{K_D^M} \qquad \text{(S11)}$$

Where K_D^U and K_D^M are the distribution ratio of the U (VI) and other competing ions in sorbent and solution, respectively

SI.5 Adsorption-desorption and cycle experiments of FCCP adsorbents

In a typical experiment, 10 mg of sorbent with U (VI) ions was added into 20 mL eluent solution (0.1 mol L^{-1}). The flasks were stirred for specified time (t, min) at room temperature, and then the solid phase was separated from the solution by centrifuge. The results were analysed with WGJ-III Trace Uranium Analyser to obtain the concentrations of U (VI) ions. The elution rate of U (VI) ions was calculated. Repeat this experiment operation for five times.

SI1. Characterization of composites

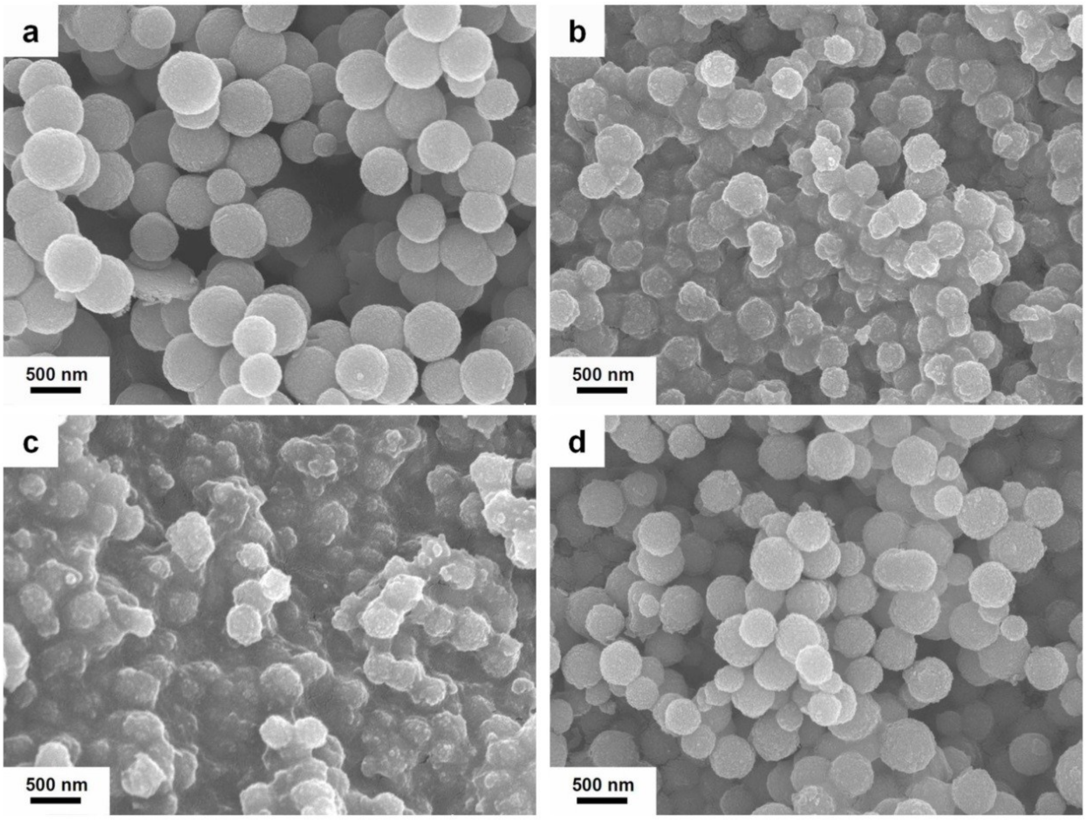

Figure S1. SEM images of the naked Fe_3O_4 (a) and FCS composites with different composition ratios (CMC: CS : Fe^{3+}) (b) 1 : 1 : 1 (c) 2 : 1 : 1; (d) 1:2:1.

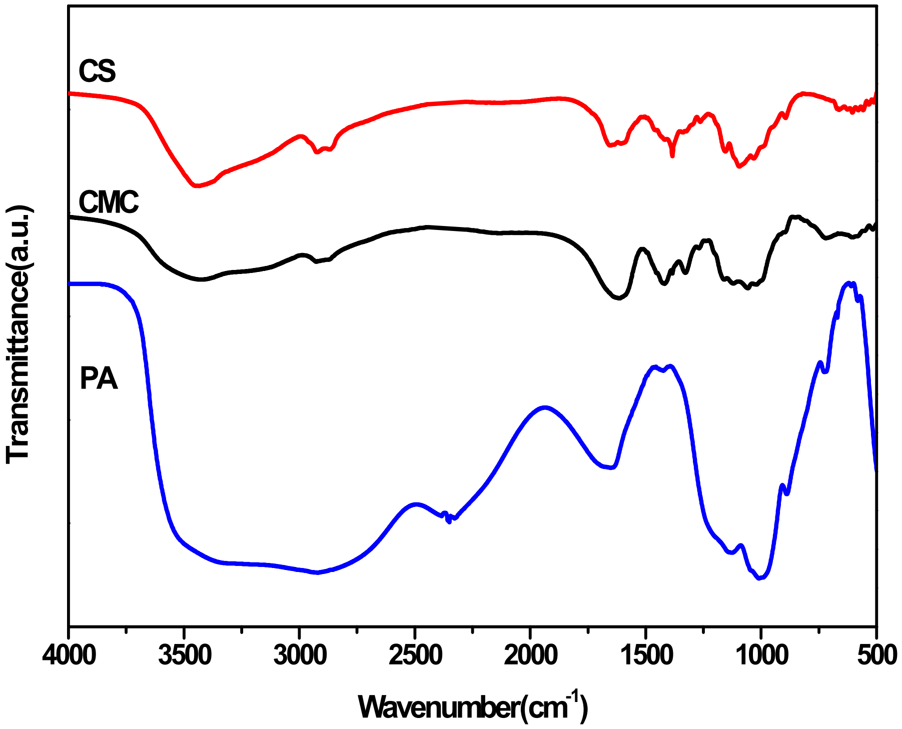

Figure S2. The FTIR spectra of pure CS, CMC and PA.

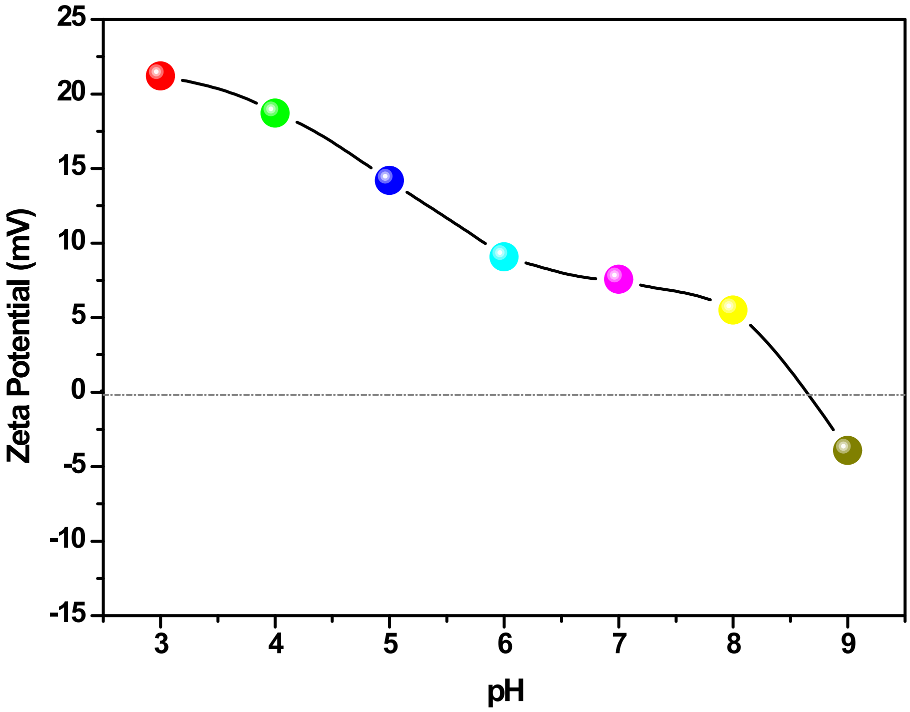

Figure S3. The Zeta potential of FCCP composites.

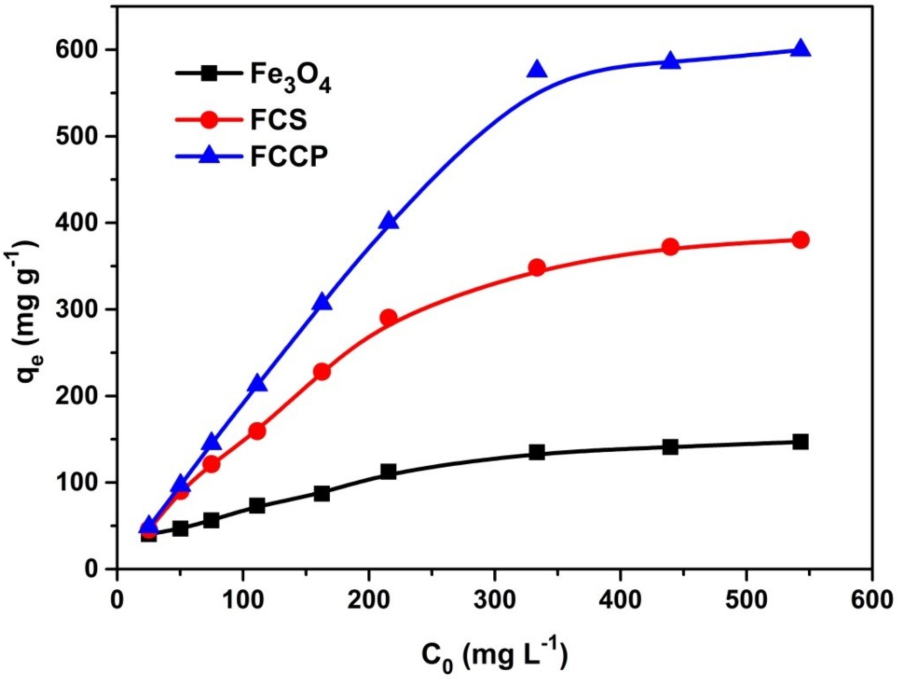

Figure S4. Effect of concentration of U(VI) on adsorption capacities of Fe_3O_4, FCS and FCCP composites, pH = 8.00; T = 25 ^{o}C; V = 20 mL; amount of adsorbent 0.01 g.

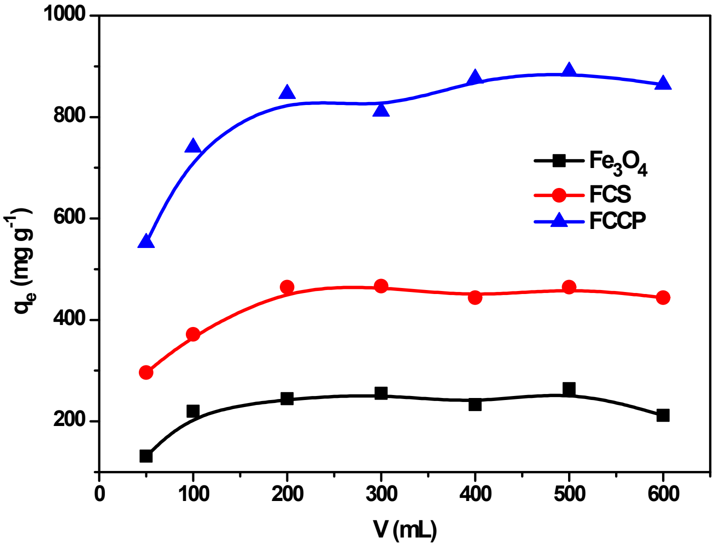

Figure S5. Effect of volume of U (VI) on adsorption capacities of Fe_3O_4, FCS and FCCP composites, pH = 8.00; T = 25 °C; amount of adsorbent 0.01 g.

Table S1 Isotherm parameter for adsorption of U(VI)

Materials	Temp (℃)	Freundich			Langmuir		
		n	k(L g^{-1})	R^2	q_m(mg g^{-1})	b(L mg^{-1})	R^2
FCS	25	2.39	40.00	0.948	413.22	0.03	0.993
	35	2.38	41.28	0.943	421.94	0.04	0.991
	45	2.49	48.99	0.964	450.45	0.04	0.993
FCCP	25	2.43	90.18	0.871	625.00	0.11	0.998
	35	2.61	106.91	0.815	628.93	0.15	0.999
	45	2.66	123.23	0.845	649.35	0.22	0.999

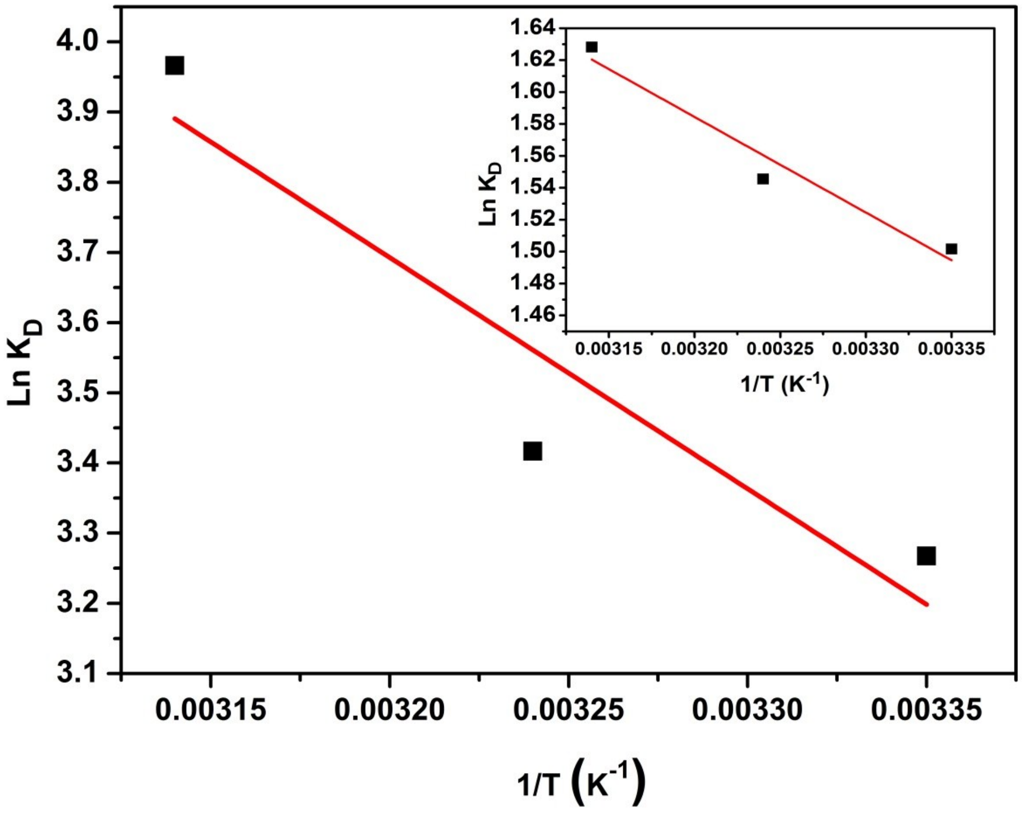

Figure S6. The influence of temperature on the U(VI) sorption for the FCCP (insert shows FCS) relationship curve between ln K_D and 1000/T (1000/K). pH= 8.0; T= 25 °C.

Table S2 The thermodynamic parameters of FCS and FCCP for U (VI) adsorption

Adsorption	ΔG^0 (kJ mol^{-1})			ΔH^0	ΔS^0
	25℃	35℃	45℃	(kJ mol^{-1})	(J mol^{-1} K^{-1})
FCS	-3.72	-3.96	-4.31	4.98	29.11
FCCP	-8.09	-8.75	-10.49	27.41	118.4

Table S3 XPS of original data for FCCP and FCCP-U

Materials	Element	Binding energy (eV)	
FCCP	O 1s	531.67	
	N 1s	399.09	
FCCP-U	O 1s	532.39	
	N 1s	399.77	
	U 4f	393.28	382.38

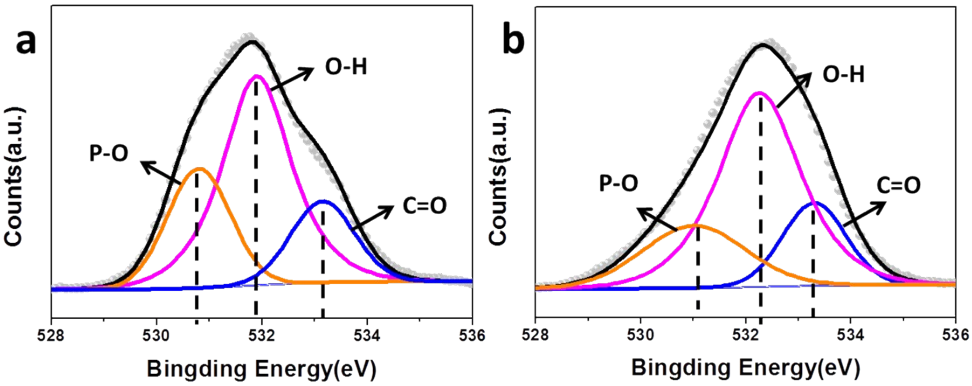

Figure S7. High resolution scans of O 1s spectra before (a) and after (b) U (VI) uptake.

Table S4 The selectivity coefficients of U for coexisting ions on the adsorbent.

	Na	K	Mg	Ca	Co	Ni	Ba	Sr	U
q_e (mg/g)	8.00	1.78	0.66	11.32	2.10	2.62	22.30	3.60	355.98
K_D	74.77	43.34	30.65	200.99	58.30	66.45	264.94	52.61	10983.65
$S_{U/M}$	146.91	253.43	358.30	54.65	188.40	165.30	41.46	208.78	

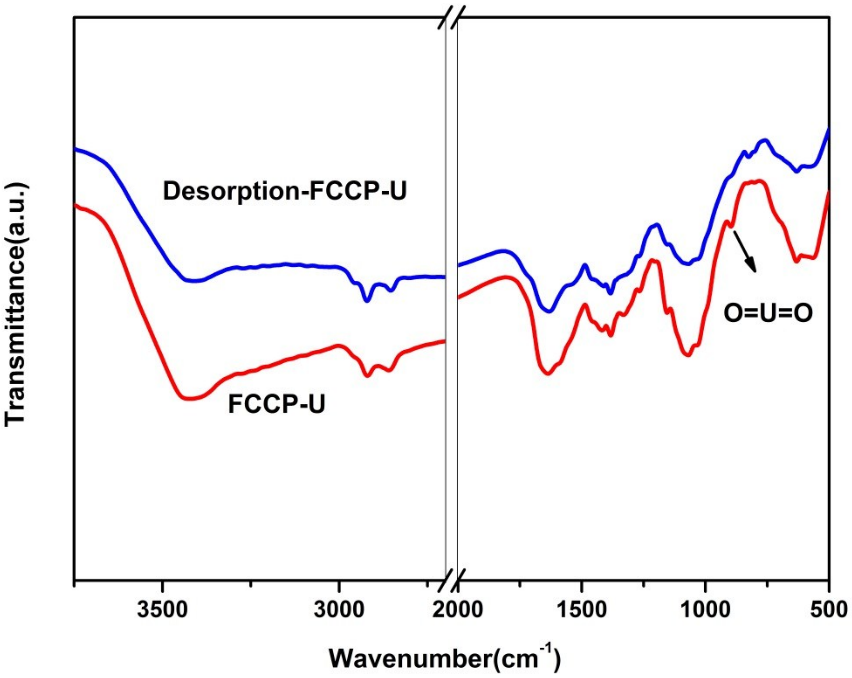

Figure S8. FTIR spectroscopy of adsorption-desorption of U (VI) for FCCP composites with 5 cycles.

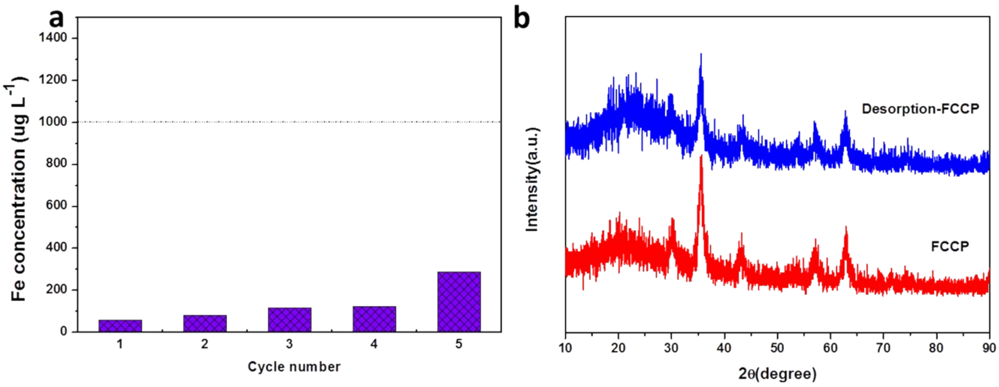

Figure S9. The leaching concentration of Fe in adsorption-desorption experiment (a); the XRD of FCCP and desorption-FCCP composites after 5 cycles (b).